Research Square

Preprints are preliminary reports that have not undergone peer review.
They should not be considered conclusive, used to inform clinical practice,
or referenced by the media as validated information.

Anti-echinococcal effect of verapamil involving regulating calcium/calmodulin-dependent protein kinase Ⅱ response *in vitro* and in a murine infection model

Hai-Jun Gao
School of Basic Medical Sciences, Lanzhou University
Xu-Dong Sun
School of Basic Medical Sciences, Lanzhou University
Yan-Ping Luo
School of Basic Medical Sciences, Lanzhou University
Hua-Sheng Pang
National Health Commission Key Laboratory of Echinococcosis Prevention and Control, Xizang Center for Disease Control and Prevention
Xing-Ming Ma
School of Basic Medical Sciences, Lanzhou University
Ting Zhang (zhangting@nipd.chinacdc.cn)
National Institute of Parasitic Diseases, China CDC
Tao Jing
School of Basic Medical Sciences, Lanzhou Univeristy
Wei Hu
National Institute of Parasitic Disease, Chinese Center for Disease Control and Prevetion
Yu-Juan Shen
National Institute of Parasitic Diseases, Chinese Center for Disease Control and Prevetion
Jian-Ping Cao
National Institute of Parasitic Diseases, Chinese Center for Disease Control and Prevetion, WHO Collaborating Center for Tropical Diseases, National Center for International Research on Tropical Diseases, Key Laboratory of Parasitie and Vector Biology of the Chinese Ministry of Health

---

Research

Keywords: Verapamil, Echinococcus, Calmodulin, Calcium-calmodulin-dependent protein kinases

Posted Date: November 13th, 2020

DOI: https://doi.org/10.21203/rs.3.rs-107151/v1

License: This work is licensed under a Creative Commons Attribution 4.0 International License.
Read Full License

Version of Record: A version of this preprint was published at Parasites & Vectors on February 15th, 2021.
See the published version at https://doi.org/10.1186/s13071-021-04618-4.

Abstract

Background: Echinococcosis caused by the larval stage of cestode of the genus *Echinococcus* is a parasitic zoonosis, imposing serious threat on the health of humans and animals globally. Albendazole is the drug of choice for treatment of echinococcosis, but it is difficult to meet the clinical challenge in chemotherapy due to its low curative rate and severe side effects. Hence, novel anti-parasitic targets and effective treatment alternatives are urgently needed. Previous study has showed that verapamil can suppress the growth of *Echinococcus granulosus* (*E. granulosus*) larva, but the mechanism remains unclear. The aim of the present study is to gain insight into the anti-echinococcal effect of verapamil on *Echinococcus* with particular focus on the regulatory role of verapamil to calcium/calmodulin-dependent protein kinase □ (Ca^{2+}/CaM-CamK □) in infected mice.

Methods: The anti-echinococcal effect of verapamil on *E. granulosus* protoscolex (PSCx) *in vitro* and *Echinococcus multilocularis* (*E. multilocularis*) metacestodes in infected mice were assessed. The morphological alteration of *Echinococcus* spp. induced by verapamil was observed by scanning electron microscope (SEM), and the changes of calcium content in both parasite and mice sera and livers were measured by SEM-energy dispersive spectrometer, inductively coupled plasma mass spectrometry and alizarin red staining accordingly. Additionally, the changes on the protein and mRNA levels of CaM and CamK □ in infected mice, and on the mRNA levels of *CamK □* in *E. granulosus* PSCx after treatment of verapamil were evaluated by immunohistochemistry or/and real-time quantitative polymerase chain reaction (RT-qPCR).

Results: *In vitro*, *E. granulosus* PSCx could be killed by verapamil at 0.5 μg/mL or more within 8 days. Under these conditions, the ultrastructure of PSCx was damaged and accompanied with obvious calcium loss and down-regulation of *CamK □* mRNA. *In vivo*, the weight and the calcium content of *E. multilocularis* metacestodes from the mice were reduced after treatment with verapamil at 40 mg/kg, meanwhile, an elevation of calcium content in the serum and liver of infected mice was observed. In addition, down-regulation of both the over-expressed CaM and CamK □ proteins and mRNAs in the liver of mice infected with *E. multilocularis* metacestodes were found after treatment of verapamil.

Conclusions: Verapamil exerted a parasiticidal activity on *Echinococcus* both *in vitro* and *in vivo* through down-regulation of Ca^{2+}/CaM-CamK □ that was over-activated by parasitic infection. It has been speculated that the Ca^{2+}/CaM-CamK □ can be a novel drug-target and verapamil is shown to be a potential anti-echinococcal drug for controlling echinococcosis in the future.

Background

Echinococcosis, a serious but neglected helminthic zoonosis, is caused by the *genus Echinococcus*, mainly involving *Echinococcus granulosus* (*E. granulosus*) that causes cystic echinococcosis (CE) and *Echinococcus multilocularis* (*E. multilocularis*) that causes alveolar echinococcosis (AE) [1]. CE is distributed globally, while AE is distributed in the northern hemisphere, bringing heavy burden of disease

[2]. According to the previous data of central Asia, at least 270 million people are being exposed to *Echinococcus*, and its prevalence in some Tibetan area of western China ranged as high as from 0.8–11.9% [3]. More notably, a higher pathogenicity and case fatality rate were associated with AE due to its tumor-like growth property [3]. The clinical treatment strategies associated with echinococcosis include surgical operation and drug chemotherapies. Among the chemotherapeutic agents, albendazole (ABZ), one of the benzimidazole derivatives, is the prime chemotherapeutic drug used for treating human echinococcosis [4], and exerts an anti-parasitic efficacy by disrupting the microtubule polymerization and biochemical processes, such as glucose and energy metabolism of the parasite [5]. However, ABZ merely exerts the parasitostatic rather than parasitocidical effects [6], and has poor gastrointestinal absorption and severe side effects [7, 8]. Hence, new drugs against this parasitosis have been investigated, such as traditional Chinese medicine from some botanical extracts [9], antineoplastic chemotherapeutics [7, 10], immunosuppressants [11, 12] and so on. However, it is disappointing that only a few of these agents, such as mefloquine or amphotericin B alone or combined with nitazoxanide, were used in auxiliary treatment for human echinococcosis [6]. Therefore, there is an urgent need to explore novel anti-*Echinococcus* drugs and drug-targets.

Ca^{2+}, a pivotal second messenger, controls the physiological process of cell, such as the proliferation, differentiation and migration [13]. The complex of Ca^{2+} and calmodulin (CaM) can specifically bind to CaM-dependent protein kinases (CamKs, including CamK Ⅰ, CamK Ⅱ, CamK Ⅳ and CamK Ⅴ) to construct the Ca^{2+}/CaM-CamKs cascade that can turn on the signal transduction process of cells [14]. Previous studies in tumors have shown that Ca^{2+}/CaM-CamKs cascade controls tumourigenesis and tumor progression [13, 15, 16]. Furthermore, Ca^{2+}/CaM-CamKs cascade has been proved to be closely related to the pathogenesis of many hepatic parasites. For example, in *Schistosoma mansoni*, an IQ-motif of SmCav1B, which is a voltage-gated calcium channel, can interact with two calmodulins (CaMs) SmCaM1 and SmCaM2 for promoting the growth process [17], and RNAi silencing of calcium-regulated protein affects the morphology and vitality of *Schistosoma japonicum* [18]. Two voltage-gated calcium channel β-subunits, $CsCa_V\beta1$ and $CsCa_V\beta2$, have boosted the parasiticidal effect of praziquantel on *Clonorchis sinensis* [19], and as well, in *Fascida hepatica*, *Fh*CaMs dyshomeostasis could obviously block its growth and motility [20]. Therefore, Ca^{2+}/CaM-CamKs has become a potential therapeutic target in cancers and parasitosis, and calcium channel inhibitors, such as verapamil and praziquantel, were confirmed to exhibit anti-tumorigenic and anti-parasitic effects [13, 15, 21, 22]. Further, verapamil has been shown to alleviate atrial fibrillation in rats by down-regulating the over-activation of Cav1.2-CaM-CaMK Ⅱ [23]. In *E. granulosus* PSCx, calcareous corpuscles have supported the necessity of calcium sources for hydatid cyst development [24], and calcium level in hydatid cyst is shown to be higher than that in the serum or plasma of host [25]. Old documents showed that verapamil is preliminary confirmed to suppress the growth of *E. granulosus* larva [26, 27], but it is unclear if the compound also had similar anti-parasitic functions on *E. multilocularis* that is a tumor-like and more harmful parasite to humans. The mechanism of verapamil against *Echinococcus* has never been investigated, and it is unclear if the inhibitory effects of verapamil on *E. granulosus* should be processed by regulating Ca^{2+}/CaM-CamK Ⅱ. Hence, this study aimed to investigate the efficacy and the possible mechanism of verapamil against *Echinococcus*.

Methods

Biochemical reagent

Verapamil (V111249), ABZ (A131023), albendazole sulfoxide (ABZ-SO, 35395) and pentobarbital sodium were purchased from Sigma (Missouri, US) and Aladdin (Shanghai, China), respectively. Antibody and PCR-primers were purchased from Abcam (Cambridge, US) and Beijing Genomics Institute (Beijing, China). ELISA kits of CaM and CaMK Ⅱ were purchased from CUSABIO (Wuhan, China). All culture reagents were purchased from Gibco (Wisent, Canada). Extraction kits of total RNA and PCR kits were purchased from Takala (Tokyo, Japan).

Separation and culture of *E. granulosus* PSCx *in vitro*

E. granulosus PSCx were obtained from naturally infected sheep liver in the slaughterhouse of Xining City, Qinghai Province, China, and then were rinsed with phosphate buffered saline (PBS) and resuspended with Dulbecco's modified Eagle's medium (DMEM) containing 1% penicillinan- streptomycin (P-S), and then incubated in 24-well culture plates (100 PSCx per well) at 37 °C, 5% CO_2. The morphological alterations of all PSCx were observed under an inverted microscope (BX43, Olympus, Japan), and the survival rate of PSCx was recorded daily.

Mouse infected with *E. multilocularis*

All experimental Kunming mice aged 6–8 weeks were purchased from the Laboratory Animal Center of Lanzhou University and maintained in a HEPA-filtered and temperature-controlled light/dark cycle environment at 22–25 ºC. The mice were fed with rodent diet (Beijing Keao, Beijing, China) ad libitum in specific pathogen-free (SPF) laboratory conditions. *E. multilocularis* PSCx were aseptically isolated from the anesthetized *E. multilocularis* infected gerbil in our lab as described previously [28], with purpose to establish the murine infection model by in situ surgical intrahepatic implantation. The healthy mice (n = 15) were infected with *E. multilocularis* PSCx (1500 PSCx per mouse) in SPF lab, and other mice (n = 5) merely with a sham operation, i.e., the uninfected group, were raised under same conditions.

Drug treatment *in vitro*

The experimental groups were divided into (i) the vehicle group with 0.1% DMSO (n = 3), (ii) the ABZ-SO group with 40 and 20 μg/mL, wherein the ABZ-SO was resolved in 0.1% DMSO (n = 3), and (iii) the verapamil group with different concentrations of 100, 80, 40, 20, 10, 5, 2, 1 and 0.5 μg/mL (n = 3). *E. granulosus* PSCx on post-treatment with drugs were stained with 0.4% trypan blue for 10 min to observe the morphological changes. In addition, other *E. granulosus* PSCx were fixed with 4% glutaraldehyde, rinsed with PBS (1×), stained with 2% osmium tetroxide for 2 hours and 1% uranyl acetate for 30 min. Subsequently, these specimens were dehydrated serially by increasing the concentrations of ethanol, dried naturally and then coated with gold as described [28]. Finally, the microstructure of PSCx was observed under a scanning electron microscope (SEM, JSM-5600LV, JEOL, Japan).

Drug treatment *in vivo*

On post-infection of *E. multilocularis* PSCx for 3 months, all *E. multilocularis* infected mice were grouped for orally administered drug therapy: (i) the infected mice were treated daily with only honey/PBS (1:1 v/v) (n = 5), (ii) ABZ mice were treated daily with 40 mg/kg ABZ in honey/PBS (1:1 v/v) (n = 5), (iii) verapamil mice were treated daily with 40 mg/kg verapamil in honey/PBS (1:1 v/v) (n = 5), and (iv) the uninfected mice were merely treated daily with honey/PBS (1:1 v/v) (n = 5). After 4 months post-treatment, *E. multilocularis* cysts, serum and liver were collected from the mice for testing the calcium content, and protein and mRNA expression of *CaM and CamK* genes.

Calcium content analysis by ICP-MS, SEM-EDS and alizarin red staining

i. Inductively coupled plasma mass spectrometry (ICP-analysis: Equal tissues or serum/culture supernatant were prepared for calcium Tissue digestion was done in a microwave digestion system using UltraClave (Milestone, Sorisole, and the sample detection was processed as described previously [29].
ii. Scanning electron microscope-energy dispersive X-ray spectroscopy (SEM-Analysis: The changes in calcium content in the *E. granulosus* PSCx and in germinal layer cells of *E. multilocularis* metacestodes after treatment of verapamil were observed by a LEO Gemini Field Emission Gun-Scanning Electron Microscope (FEG-SEM, JEOL, Japan) as described previously [30].
iii. Alizarin red staining analysis: *E. multilocularis* metacestodes and mice liver were fixed with 4% paraformaldehyde for 2 weeks, and then stained with alizarin red to detect the calcification as described previously [31]. The images were analyzed by using Image J software (National Institutes of Health, Bethesda, MD, USA) to calculate the percentage of positively stained calcium deposits in the image field.

CaM and CamK protein expression analysis by IHC-P

i. Paraffin-immunohistochemistry (IHC-tests: 4 μm thick sections of *E. multilocularis* metacestodes and mouse liver were processed for evaluating CaM or CamK expression as described previously [32, 33], followed by immunoreaction using rabbit anti-CaM/CamK antibody (Bioss, Beijing, China) at 1:300/1:200 and secondary antibody (Goat anti-rabbit IgG, Bioss, Beijing, China) at 1:800. Finally, the slides were viewed under a fluorescence microscope (Olympus, Japan). The semi-quantified analysis was evaluated by using Image J software.
ii. ELISA tests: The serum and tissue samples were added to PBS (pH = 7.containing PMSF (10 mM/L), followed by rapid homogenization and centrifugation at 1000 · *g* for 10 min to investigate the concentrations of CaM and CamK proteins according to the ELISA kit protocols.

CaM and *CamK* mRNA analysis by RT-qPCR

The expression of *CaM* or/and *CamK* mRNA in *E. granulosus* PSCx, mice liver and *E. multilocularis* cysts were tested by real-time quantitative polymerase chain reaction (RT-qPCR), and *β-actin* mRNA was

used as an internal standard. Nucleic acid in different tissues was isolated by using Trizol reagent (Invitrogen, San Diego, USA), and then reverse-transcribed to cDNA, and amplification of cDNA was performed by RT-qPCR as described by Takara kit protocols (No. RR036A). The primers used were as follow: *Eg-CamK Ⅱ/Em-Camk Ⅱ* (forward, 5′-TCGTTGTTCAAGTCGGTTCG-3′; reverse, 5′-GGTGCTGAGA

GACCCACTAG-3′), *Eg-β-actin/Em-β-actin* (forward, 5′-AGACATCAGGGAGTGATGGTT

-3′; reverse, 5′- GAGGACTGGATGCTCCTCAGG-3′); *mouse-CamK Ⅱ* (forward, 5′-GGCC

TGGACTTT-CATCGATTCTA-3′; reverse, 5′-CATCAGGTGGATGTGAGGGTTC-3′), *mouse-CaM* (forward, 5′-AAGCCGAGCTGCAGGATATGA-3′; reverse, 5′-CAGTTCTGCC

GCACTGATGTAA-3′), *mouse-β-actin* (forward, 5′-TTGTTACCAACTGGGACG-3′; reverse, 5′-GGCATAGAGGTCTTTACGG − 3′).

Statistical analysis

The data were presented as means ± standard deviation (SD). Statistical differences among different groups were assessed by T test and paired comparisons. Statistical analysis was performed by SPSS version 22.0 (IBM Corp., Chicago, USA) and GraphPad Prism version 7.0 (GraphPad Software, Inc., San Diego, CA, USA). $P < 0.05$ indicated statistical significant differences.

Results

Effect of verapamil on *E. granulosus* PSCx *in vitro*

The survival rate of *E. granulosus* PSCx after treatment with a series of concentrations of verapamil at 0.5, 1, 2, 5, 10, 20, 40, 80 and 100 μg/mL within 8 days was shown in Fig. 1A. The mortality rate of PSCx showed a time-dependent property when exposed to 0.5–40 μg/mL verapamil, and all PSCx were killed within 2 days at 40 μg/mL or 4 days at 20 μg/mL. However, ABZ-SO merely killed 13% PSCx on day 2 at 40 μg/mL or 21% on day 4 at 20 μg/mL, and 4% PSCx were dead on day 2 or 8% on day 4 in the vehicle group.

The results of light microscope showed when compared to the natural morphology of PSCx in the vehicle group and mild alterations of PSCx in ABZ-SO (20 μg/mL) group, an obvious morphological alterations (i.e. disappearance of calcareous corpuscles) of PSCx was observed after exposed to verapamil 20 μg/mL for 4 days, (Fig. 1Ba-c). In addition, PSCx in verapamil (20 μg/mL) group on day 4 was dyed with trypan blue, unlike the viable PSCx in ABZ-SO (20 μg/mL) group or vehicle group (Fig. 1Bd-f). The ultrastructural destructure in PSCx, involving the shedding of the tegument, the disappearance of the hooks and the presence of numerous blebs, were observed by SEM when exposed to verapamil (20 μg/mL) for 4 days, while that in the vehicle group or in ABZ-SO (20 μg/mL) group were still shown to be intact (Fig. 1Bg-i).

Changes of calcium content in *E. granulosus* PSCx exposed to verapamil *in vitro*

The calcium distribution in *E. granulosus* PSCx when treated with verapamil (20 μg/mL) for 4 days has become heterogeneous and sparse as compared with that in the vehicle group by SEM-EDS (Fig. 2A). The semi-quantitative analysis showed that the calcium level in PSCx was decreased after treatment of verapamil (Fig. 2B). In addition, compared with the vehicle group, an obvious drug-dose dependent increase of the calcium content in the culture supernatant of the verapamil group was observed (Fig. 2C).

Effect of verapamil on *E. multilocularis* metacestodes *in vivo*

E. multilocularis infected mice were treated with verapamil (40 mg/kg) or ABZ (40 mg/kg) for 4 months *in vivo*. The wet weight of *E. multilocularis* cysts from the verapamil (0.98 ± 0.33 g) or ABZ group (1.04 ± 0.14 g) showed significant declination when compared with that from the infected group (5.90 ± 0.75 g) (P = 0.000, Table 1).

Table 1
The changes of wet weight of *E. multilocularis* metacestodes in mice after treatment of verapamil for 4 months

Group	No. of mice	Dose	Cysts weight (g) (Mean ± SD)
Infected	5	NA	5.90 ± 0.75
ABZ	5	40 mg/kg/day	1.04 ± 0.14*
Vepm	5	40 mg/kg/day	0.98 ± 0.33*

Changes of calcium concentration in *E. multilocularis* infected mice after verapamil treatment

The calcium concentration of serum in *E. multilocularis* infected mice was 4.92 ± 0.77 mg/L, which was declined by 2-folds when compared with the uninfected group (9.89 ± 1.92 mg/L), while post-treatment with verapamil for 4 months showed the recovery of calcium concentration to 6.39 ± 0.79 mg/L (Table 2). Similarly, the level of calcium in the liver of mice was declined from 296.72 ± 9.43 mg/L to 172.72 ± 16.63 mg/L due to *E. multilocularis* metacestodes infection. Interestingly, the calcium content in the liver was increased to 226.78 ± 43.93 mg/L after treatment of verapamil (P = 0.009). Additionally, ICP-MS assay showed that the calcium level in *E. multilocularis* cysts from the infected group was 3182.28 ± 190.77 mg/L, which was merely decreased to 3013.98 ± 115.80 mg/L after treatment of verapamil for 4 months (P = 0.13). Furthermore, calcium changes in *E. multilocularis* cysts were evaluated by SEM-EDS (Fig. 3A), and the percentage of calcium weight in *E. multilocularis* cysts demonstrated a swift drop from 14.28–8.66% after treatment with verapamil, showing statistical significant differences (P = 0.000) (Fig. 3B). Alizarin red staining showed that calcium deposition around the portal area of the liver in the

infected mice was increased significantly when compared with that in the uninfected group (Fig. 4). The loss of calcium content in the infected livers showed no apparent recovery after treatment of verapamil, and meanwhile in *E. multilocularis* cysts, no obvious reduce of calcium content was observed ($P > 0.05$), but the reduce in the number of PSCx was observed.

Table 2
ICP-MS analysis of calcium content in *E. multilocularis* infected mice after treatment of verapamil for 4 months

Samples	Calcium concentration (mg/L)		
	Uninfected group	Infected group [a]	Vepm group [b]
Serum	9.89 ± 1.92	4.92 ± 0.77*	6.39 ± 0.79
Liver	296.72 ± 9.43	172.72 ± 16.63*	226.78 ± 43.93*
Cysts	NA	3182.28 ± 190.77	3013.98 ± 115.80

Analysis of CaM and CamK□ protein in *E. multilocularis* infected mice treated with verapamil

IHC-P staining exhibited high expression of CaM in the liver of the infected group when compared with that in the uninfected group (Fig. 5A), but the pathological progression could be inhibited by verapamil, showing statistical significant differences ($P < 0.05$). Furthermore, ELISA assay showed that the CaM protein concentration in mouse serum or liver increased significantly from 13.81 ± 1.65 to 22.25 ± 5.55 μg/mL or from 3.42 ± 0.27 to 6.06 ± 1.83 μg/mL after *E. multilocularis* infection, but after treatment with verapamil, an obvious inhibitory effect on CaM protein expression was observed in the serum (8.13 ± 1.26 μg/mL) and liver (1.60 ± 0.68 μg/mL) not in the cysts from 2.36 ± 0.87 to 1.68 ± 0.10 μg/mL (Table 3).

Table 3
ELISA analysis of CaM and CamK □ protein in *E. multilocularis* infected mice under oral administration of verapamil for 4 months

Indexes	Samples	Uninfected group	Infected group [a]	Vepm group [b]
CaM (μg/mL)	Serum	13.81 ± 1.65	22.25 ± 5.55*	8.13 ± 1.26*
	Liver	3.42 ± 0.27	6.06 ± 1.83*	1.60 ± 0.68*
	Cysts	NA	2.36 ± 0.87	1.68 ± 0.10
CamK□ (ng/mL)	Serum	5.88 ± 0.99	22.87 ± 4.23*	5.13 ± 1.74*
	Liver	2.00 ± 0.61	4.25 ± 1.84*	1.97 ± 0.56*
	Cysts	NA	2.65 ± 1.24	1.79 ± 0.36

Similar to CaM, IHC-P assay supported that the over-expression of CamK Ⅱ of the liver and cysts in *E. multilocularis* infected mice were significantly suppressed by verapamil treatment (Fig. 5B). In addition, the increase of CamK Ⅱ content in mice serum (22.87 ± 4.23 ng/mL) and liver (4.25 ± 1.84 ng/mL) were observed after *E. multilocularis* infection, and then were decreased to 5.13 ± 1.74 ng/mL and 1.97 ± 0.56 ng/mL after treatment of verapamil. However, only a mild decrease of CaMK Ⅱ content in cysts (from 2.65 ± 1.24 to 1.79 ± 0.36 ng/mL) was observed after verapamil treatment ($P > 0.05$, Table 3).

Analysis of *CaM* and *CamK Ⅱ* mRNA in parasite and *E. multilocularis* infected mice after treatment with verapamil

To further observe the change of Ca^{2+}/CaM-CamK Ⅱ in parasite infected mice after treatment of verapamil, the change in *CaM* or/and *CamK Ⅱ* mRNA of mice liver and *Echinococcus* were evaluated by using RT-qPCR. Figure 6A-B showed that *CaM* and *CamK Ⅱ* mRNA expression in mice liver obviously increased by 4-fold and 6-fold after infection of *Echinococcus*. Nonetheless, the over-expression of *CaM* and *CamK Ⅱ* mRNA in the liver were significantly suppressed by verapamil ($P = 0.000$). Meanwhile, in the cysts after treatment of verapamil, obvious down-regulation was observed in *CamK Ⅱ* mRNA expression not in *CaM* mRNA expression with mild reduce ($P > 0.05$). Furthermore, in *E. granulosus* PSCx exposed to verapamil *in vitro*, obvious down-regulation of *CamK Ⅱ* mRNA expression was observed (Fig. 6C).

Discussion

E. granulosus and E. multilocularis metacestodes are inclined to be parasite on the liver, and *E. multilocularis* metacestodes with tumor-like growth property has become more noticeable and leads to death if untreated [34]. While accompanied with poor intestinal absorption and heavy side effects [7], ABZ, exerting parasitostatic rather than parasitocidical effect, has long been used for treating for human echinococcosis. Hence, the urgency of exploring new anti-echinococcal targets and therapeutic options should be considered.

Ca^{2+}/CaM-CamKs as a potential therapeutic target in cancers and many parasitosis is closely monitored, but it is unclear as to how Ca^{2+}/CaM-CamK Ⅱ regulates the growth and development of *Echinococcus* spp. and requires urgent exploration with the purpose to find potential drugs for treating echinococcosis at early stages.

In this study, the anti-echinococcal effect of verapamil on *E. granulosus* PSCx was found to be time-dependent and dose-dependent, which was also observed when studying the anti-tumor proliferation. As is well-known, calcareous corpuscles in PSCx can persistently provide abundant calcium sources to promote PSCx development into cysts [24]. In the presented study, the rapid disappearance of calcareous

corpuscles and the loss of calcium content in *E. granulosus* PSCx were observed when exposed to verapamil, indicating that verapamil could kill *E. granulosus* PSCx by promoting calcium loss.

AE is usually named a “parasitic cancer” due to its distinctive tumor-like growth properties, and approximately 70% of the metacestodes were found in the right lobe of the patient’s liver. The germinal layer cells in *E. multilocularis* metacestodes with high regenerative capacity can develop into new multicular structures, such as PSCx, which can further develop into new metacestodes again. So, the *E. multilocularis* metacestodes can infiltrate the whole liver of host [35]. In this study, the infection model was established by in situ surgical intrahepatic implant to follow the natural occurrence and development of AE in the mouse as possible. After *E. multilocularis* infected mice were treated with verapamil 40 mg/kg for 4 months, the weight of *E. multilocularis* cysts was decreased significantly, suggesting that the growth of metacestodes was suppressed. This was similar to the results of Cao’s observation of verapamil on CE mice [26]. It was reported that the infection of *E. multilocularis* metacestodes reduced serous calcium levels in both mice and humans [25, 36]. Interestingly, our results discovered that the reduction of calcium content in *E. multilocularis* infected mice was significantly recovered under administration of verapamil, and the apparent suppression was observed in liver rather than in serum or cysts with mild increase. The calcium content in *E. multilocularis* metacestodes is much higher than that in the host liver and serum, indicating that *E. multilocularis* PSCx development into metacestodes needs continuous absorption of calcium from the host. Furthermore, the results of SEM-EDS assay showed that after treatment with verapamil, both the calcium content and number of germinal layer cells were obviously reduced. Thus, we speculated that the proliferation of germinal layer cells was regulated and controlled by calcium supply in infected mice and can be broken by calcium channel inhibitor verapamil. However, the detailed mechanism of suppressing the growth of germinal layer cells by verapamil regulating Ca^{2+}/CaM-CamKs cascade needs to be further explored. Further, alizarin red staining and ICP-MS results also supported that *E. multilocularis* metacestodes could cause calcium content translocation from mice into the parasite, and calcium channel inhibitor (verapamil) would rescue the calcium loss of *E. multilocularis* infected mice. In addition, abundant lymphocytes were distributed in the liver around *E. multilocularis* cysts after treatment with verapamil, which is potentially associated with the increase of calcium content in the liver of *E. multilocularis* infected mice after treatment with verapamil, the probable reason is that enough calcium could promote the proliferation and polarization of T cells [37], but the abnormality of lymphocytes development caused by loss of calcium in *Echinococcus* infected host still requires further exploration.

We found that the increased expression of CaM and CamK Ⅱ protein in mouse serum and liver were caused by *E. multilocularis* metacestodes infection, but the over-expression of CaM and CamK Ⅱ protein were suppressed significantly by verapamil. Furthermore, the expression of *CaM* and *CamK Ⅱ* mRNA in mice liver and *E. multilocularis* metacestodes were down-regulated after treatment with verapamil. Our results partially supported Sujeevi S. K. Nawaratna’s recent findings that Ca^{2+}/CaM-CamK Ⅱ in helminth parasite are putative therapeutic targets that could provide biochemical and pharmacological information for exploring novel compounds in the future [38]. Ca^{2+}/CaM-CamK Ⅱ controls the completion of life cycle

in *Echinococcus*, and calcium channel blocker verapamil exhibits strong inhibitory effects on *Echinococcus*, including the germinal layer cell, PSCx and metacestodes. Therefore, further study should emphasize on the molecular and immune mechanisms of verapamil on the over-activated Ca^{2+}/CaM-CamK Ⅱ in *Echinococcus* infected host. On the other hand, based on Ca^{2+}/CaM-CamK Ⅱ, seeking novel anti-echinococcal drug-targets and effective treatment strategies should be carefully investigated.

Conclusions

Our study results suggested that verapamil had parasiticidal efficacy on both *E. granulosus* PSCx *in vitro* by promoting calcium loss, and *E. multilocularis* metacestodes *in vivo* by inhibiting calcium content translocating from mice to parasite. Furthermore, Ca^{2+}/CaM-CamK Ⅱ in the mouse was over-activated by *Echinococcus* infection, which was alleviated after oral administration of verapamil. Thus, our findings provide new information on identifying Ca^{2+}/CaM-CamK Ⅱ in anti-*Echinococcus* targets and the functions of verapamil as an anti-echinococcal compound. Further investigation of Ca^{2+}/CaM-CamK Ⅱ functions in the growth and development of *Echinococcus* and the chronic toxicity evaluation of verapamil are currently in progress in our laboratory.

Abbreviations

Vepm, verapamil; AE, alveolar echinococcosis; PSCx, protoscolex; ABZ, aldendazole; CaM, calmodulin; CamK Ⅱ, Ca^{2+}/calmodulin dependent protein kinase Ⅱ; ABZ-SO, albendazole sulfoxide; IHC-P, immunohistochemistry-paraffin; PBS, phosphate buffered saline; SEM-EDS, scanning electron microscope and energy dispersive spectrometer; ICP-MS, inductively coupled plasma mass spectrometry; RT-qPCR, real-time quantitative polymerase chain reaction.

Declarations

Ethics approval and consent to participate

This study was conducted in accordance with the Chinese Laboratory Animal Administration Act and the study protocol was approved by the Experimental Animal Ethics Committee of School of Basic Medical Sciences, Lanzhou University (permit no. 2014-12-003).

Consent for publication

Not applicable.

Availability of data and materials

The Datasets supporting the conclusions of this article are included within the article.

Competing interests

The authors declare that they have no competing interests.

Funding

This study was financially supported by the Foundation of National Science and Technology Major Program (Grant no. 2018ZX10713001-004), National Natural Science Foundation of China (Grant no. 81171632, 81201315), the Fundamental Research Funds for the Central Universities (Grant no. lzujbky-2014-m02) and the Foundation of Shanghai Municipal Health Commission (Grant no. 201940302) and the Non-profit Central Research Institute Fund of Chinese Academy of Medical Sciences (Grant no. 2019PT320004). The funders had no role in the study design, data collection, data analysis, data interpretation, or the writing of this report.

Authors' contributions

TJ, TZ and HJG conceived and designed the experiments; HJG and YPL performed the experiments; HJG, TZ, WH, XMM, YJS, JPC analyzed the data and contributed reagents and materials, XDS and HSP participated in animal model; HJG, TZ wrote the paper. All authors have read and approved the final version of the manuscript.

Acknowledgments

The authors would like to thank Dr. HB Zhang, B Jang and LL Huo (National Institute of Parasitic Diseases, Chinese Center for Disease Control and Prevention, Key Laboratory of Parasite and Vector Biology, MOH, National Center for International Research on Tropical Diseases, WHO Collaborating Centre for Tropical Diseases, China) for the technical assistance.

Author details

[1]School of Basic Medical Sciences, Lanzhou University, Lanzhou 730000, Gansu Province, People's Republic of China.

[2]National Institute of Parasitic Diseases, Chinese Center for Disease Control and Prevention, WHO Collaborating Center for Tropical Diseases, National Center for International Research on Tropical Diseases, Key Laboratory of Parasite and Vector Biology of the Chinese Ministry of Health, Shanghai 200025, People's Republic of China.

[3]Ganzr Tibetan Autonomous Prefecture Center for Disease Control and Prevention, Kangding 626000, Sichuan Province, People's Republic of China.

[4]National Health Commission Key Laboratory of Echinococcosis Prevention and Control, Xizang Center for Disease Control and Prevention, 21 Linkuo North Road, Lhasa 850000, Tibet Autonomous Region, People's Republic of China.

References

1. Wang H, Li J, Guo B, Zhao L, Zhang Z, McManus DP, et al. In vitro culture of *Echinococcus multilocularis* producing protoscoleces and mouse infection with the cultured vesicles. Parasit Vectors. 2016;9:411.
2. Romig T, Deplazes P, Jenkins D, Giraudoux P, Massolo A, Craig PS, et al. Ecology and Life Cycle Patterns of Echinococcus Species. Adv Parasitol. 2017;95:213-314.
3. Li ZD, Mo XJ, Yan S, Wang D, Xu B, Guo J, et al. Multiplex cytokine and antibody profile in cystic echinococcosis patients during a three-year follow-up in reference to the cyst stages. Parasit Vectors. 2020;13:133.
4. Kern P, Menezes da Silva A, Akhan O, Mullhaupt B, Vizcaychipi KA, Budke C, et al. The Echinococcoses: Diagnosis, Clinical Management and Burden of Disease. Adv Parasitol. 2017;96:259-369.
5. Horton J. Albendazole: a review of anthelmintic efficacy and safety in humans. Parasitology. 2000;121: S113-32.
6. Fabbri J, Pensel PE, Albani CM, Arce VB, Martire DO, Elissondo MC. Drug repurposing for the treatment of alveolar echinococcosis: in vitro and in vivo effects of silica nanoparticles modified with dichlorophen. Parasitology. 2019; 146:1620-30.
7. Yuan M, Luo Y, Xin Q, Gao H, Zhang G, Jing T. Efficacy of osthole for *Echinococcus granulosus* in vitro and *Echinococcus multilocularis* in vivo. Vet Parasitol. 2016;226:38-43.
8. Stamatakos M, Sargedi C, Stefanaki C, Safioleas C, Matthaiopoulou I, Safioleas M. Anthelminthic treatment: an adjuvant therapeutic strategy against *Echinococcus granulosus*. Parasitol Int. 2009;58:115-20.
9. Abdel-Baki AA, Almalki E, Mansour L, Al-Quarishy S. In Vitro Scolicidal Effects of Salvadora persica Root Extract against Protoscolices of *Echinococcus granulosu* Korean J Parasitol. 2016;54:61-6.
10. Nicolao MC, Elissondo MC, Denegri GM, Goya AB, Cumino AC. *In vitr*o and in vivo effects of tamoxifen against larval stage *Echinococcus granulosus*. Antimicrob Agents Chemother. 2014;58:5146-54.
11. Colebrook AL, Jenkins DJ, Jones MK, Tatarczuch L, Lightowlers MW. Effect of cyclosporin A on the survival and ultrastructure of *Echinococcus granulosus* protoscoleces *in vitro*. Parasitology. 2004;129:497-504.
12. Reuter S, Merkle M, Brehm K, Kern P, Manfras B. Effect of amphotericin B on larval growth of *Echinococcus multilocularis*. Antimicrob Agents Chemother. 2003;47:620-5.
13. Iamshanova O, Fiorio Pla A, Prevarskaya N. Molecular mechanisms of tumour invasion: regulation by calcium signals. J Physiol. 2017;595:3063-75.
14. Billker O, Lourido S, Sibley LD. Calcium-dependent signaling and kinases in apicomplexan parasites. Cell Host Microbe. 2009;56:612-22.

15. Cui C, Merritt R, Fu L, Pan Z. Targeting calcium signaling in cancer therapy. Acta Pharm Sin B. 2017;71:3-17.
16. Hu Y, Liu P, Kang L, Li J, Li R, Liu T. Mechanism of Marsdenia tenacissima extract promoting apoptosis of lung cancer by regulating Ca(2+)/CaM/CaMK signaling. J Ethnopharmacol. 2020;251:1125-35.
17. Thomas CM, Timson DJ. Calmodulins from *Schistosoma mansoni*: Biochemical analysis and interaction with IQ-motifs from voltage-gated calcium channels. Cell Calcium. 2018;74:1-13.
18. Zou X, Jin Y-m, Liu P-p, Wu Q-j, Liu J-m, Lin J-j. RNAi silencing of calcium-regulated heat-stable protein of 24 kDa in *Schistosoma japonicum* affects parasite growth. Parasitology Research. 2010;108 3:567-72.
19. Cho PY, Yoo WG, Kim TI, Ahn SK, Cho SH, Kim TS, et al. Molecular characterization of voltage-gated calcium channel beta-subunits of *Clonorchis sinensis*. Parasitol Res. 2014;113 1:121-9.
20. McCammick EM, McVeigh P, McCusker P, Timson DJ, Morphew RM, Brophy PM, et al. Calmodulin disruption impacts growth and motility in juvenile liver fluke. Parasit Vectors. 2016;9:46.
21. Zhao L, Zhao Y, Schwarz B, Mysliwietz J, Hartig R, Camaj P, et al. Verapamil inhibits tumor progression of chemotherapy-resistant pancreatic cancer side population cells. Int J Oncol. 2016;49 1:99-110.
22. Harun MSR, Marsh V, Elsaied NA, Webb KF, Elsheikha HM. Effects of *Toxoplasma gondii* infection on the function and integrity of human cerebrovascular endothelial cells and the influence of verapamil treatment in vitro. Brain Res. 2020;1746: 147002.
23. Zhang YT, Hu HH, Chen W, Shi S, Weng W. Influence of wenxin granule on atrial myocytes calcium-handling CaV1.2-CaM-CaMK signal pathway of atrial brillation rat. China journal of traditional Chinese medicine and pharmacy. 2017;32(5):2246-9. (in Chinese)
24. Rodrigues JJS, Ferreira HB, Farias SE, Zaha A. A protein with a novel calcium-binding domain associated with calcareous corpuscles in *Echinococcus granulosus*. Biochemical & Biophysical Research Communications. 1997; 237(2):451-6.
25. Desser SS. Calcium accumulation in larval *Echinococcus multilocularis*. Canadian Journal of Zoology. 1963; 41(6):1055-9.
26. Cao D, Bai H, Zhao H. Effects of verapamil hydrochloride on the ultrastructures of secondary cysts of *Echinococcus granulosus* in mice. Journal of parasitic biology. 2010;5(6): 448-9. (in Chinese)
27. Cao D, Shi D, Bao G. Observation on verapamil and albendazole against *Echinococcus granulosus* protoscolex *in vitro*. Endemic Disease Bulletin (China). 2004; 19(1):23-24. (in Chinese)
28. Naguleswaran A, Spicher M, Vonlaufen N, Ortega-Mora LM, Torgerson P, Gottstein B, et al. In vitro metacestodicidal activities of genistein and other isoflavones against *Echinococcus multilocularis* and *Echinococcus granulosus*. Antimicrob Agents Chemother. 2006;50 (11): 3770-8.
29. Orct T, Jurasovic J, Micek V, Karaica D, Sabolic I. Macro- and microelements in the rat liver, kidneys, and brain tissues; sex differences and effect of blood removal by perfusion in vivo. J Trace Elem Med Biol. 2017;40:104-11

30. Jung M, Jang HB, Lee SE, Park JH, Hwang YS. In vitro micro-mineralized tissue formation by the combinatory condition of adipose-derived stem cells, macroporous PLGA microspheres and a bioreactor. Macromolecular Research. 2013;22 1:47-57.
31. Mori F, Tanji K, Wakabayashi K. Widespread calcium deposits, as detected using the alizarin red S technique, in the nervous system of rats treated with dimethyl mercury. Neuropathology. 2000;20(3):210-5.
32. Xu B, Xing R, Huang Z, Yin S, Li X, Zhang L, et al. Excessive mechanical stress induces chondrocyte apoptosis through TRPV4 in an anterior cruciate ligament-transected rat osteoarthritis model. Life Sci. 2019;228:158-66.
33. Yang WR, Li BB, Hu Y, Zhang L, Wang XZ. Oxidative stress mediates heat-induced changes of tight junction proteins in porcine sertoli cells via inhibiting CaMKKβ-AMPK pathway. Theriogenology. 2020;142:104-13.
34. Maria AC, Celina EM. Efficacy of albendazole in combination with thymol against *Echinococcus multilocularis* protoscoleces and metacestodes. Acta Trop. 2014;140:61-7.
35. Diaz A, Casaravilla C, Irigoin F, Lin G, Previato JO, Ferreira F. Understanding the laminated layer of larval Echinococcus I: structure. Trends Parasitol. 2011;27 5:204-13.
36. Wang Y, Wang S, Pu Y, Zhu J, Zhao W. Observation of trace elements in serum of patients with hepatic echinococcosis. Journal of Ningxia Medical University. 2011;33(8):764-5.
37. Vaeth M, Maus M, Klein-Hessling S, Freinkman E, Yang J, Eckstein M, et al. Store-Operated Ca(2+) Entry Controls Clonal Expansion of T Cells through Metabolic Reprogramming. Immunity. 2017;47 4:664-79.
38. Nawaratna SSK, You H, Jones MK, McManus DP, Gobert GN. Calcium and Ca(2+)/ Calmodulin-dependent kinase II as targets for helminth parasite control. Biochem Soc Trans. 2018;46(6):1743-51.

Figures

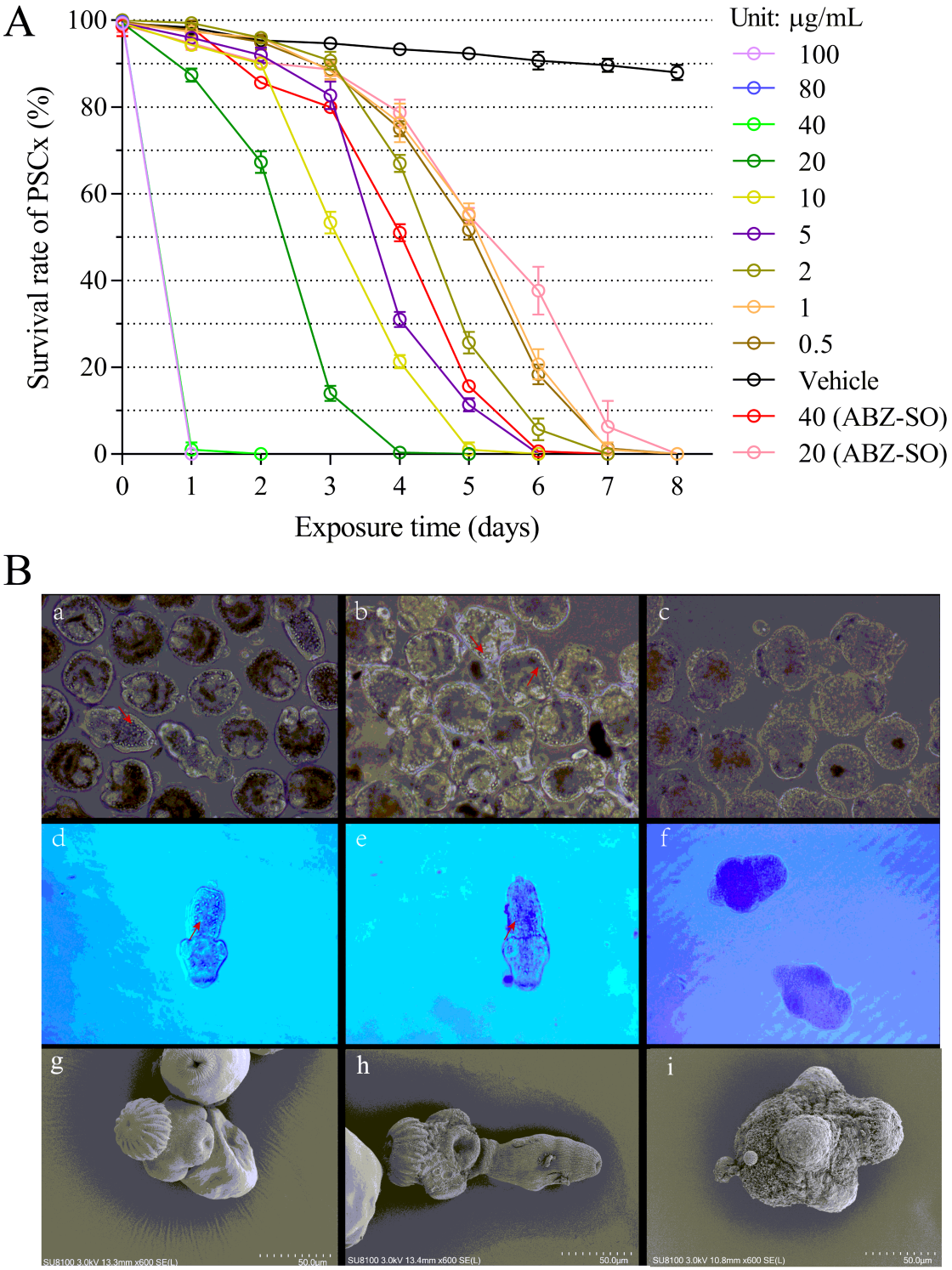

Figure 1

The effect of verapamil against E. granulosus protoscolex in vitro. A. E. granulosus protoscolex (PSCx) exposed to verapamil (vepm) at 100 to 0.5 μg/mL, ABZ-SO of 40 and 20μg/mL and 0.1% DMSO (the vehicle group) within 8 days. B. The morphological changes and ultrastructural alterations of PSCx exposed to different drugs for 4 days were observed under light microscope and SEM. a, d, g The typical morphology and structural integrity of PSCx from the vehicle group; b, e, h The mild morphological and

structural alterations in ABZ-SO (20 μg/mL) group. c, f, j Obvious morphological and ultrastructural destructures in PSCx exposed to vepm (20 μg/mL), the disappearance of calcareous corpuscles and hooks, shedding of the tegument and the presence of numerous blebs. a-c Light microscope without any staining (200 × magnification); d-f Light microscope with trypan blue staining (200 × magnification); g-i SEM (600 × magnification). Arrowhead (red) indicates intact calcareous corpuscle.

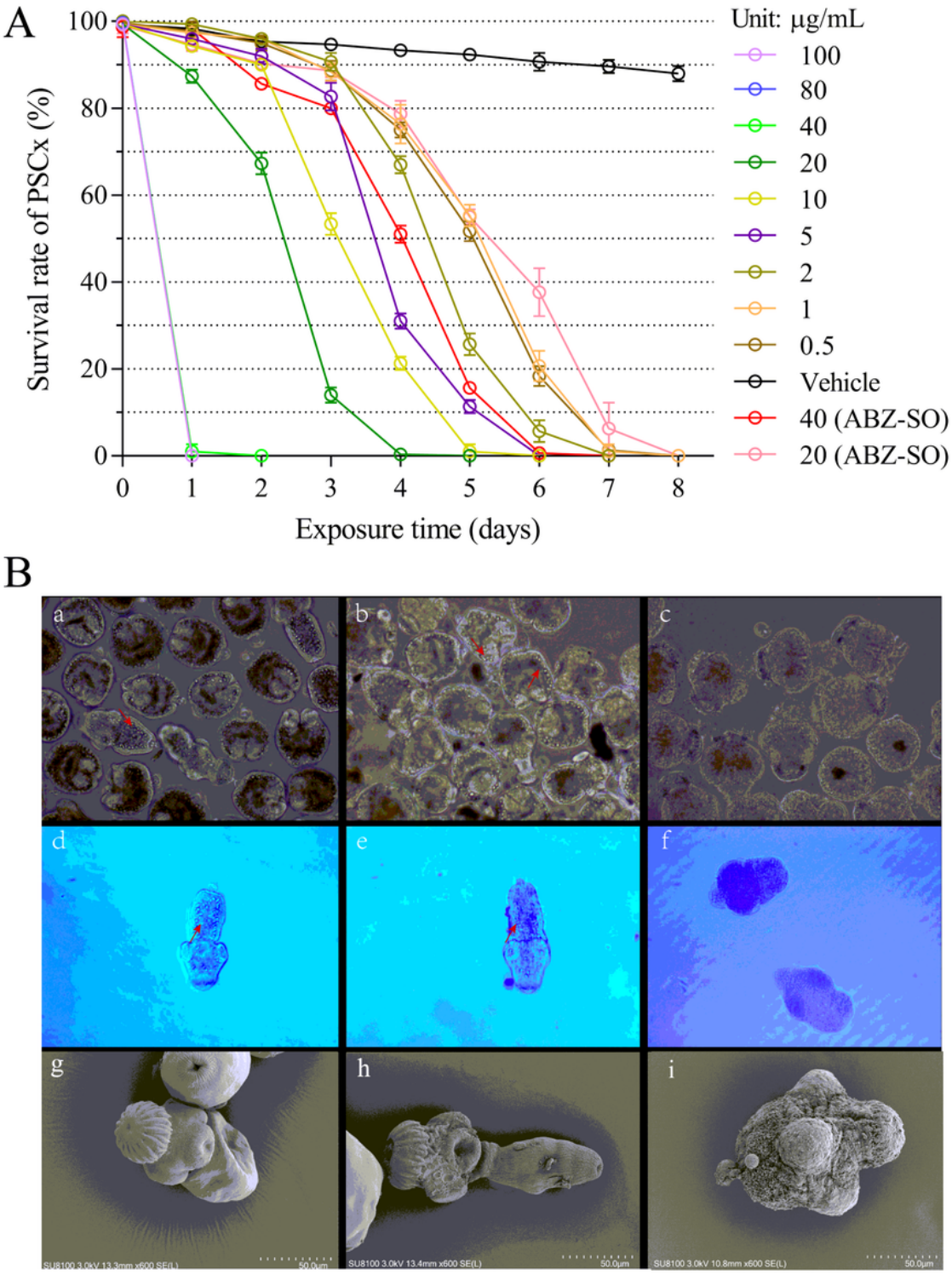

Figure 1

The effect of verapamil against E. granulosus protoscolex in vitro. A. E. granulosus protoscolex (PSCx) exposed to verapamil (vepm) at 100 to 0.5 μg/mL, ABZ-SO of 40 and 20μg/mL and 0.1% DMSO (the vehicle group) within 8 days. B. The morphological changes and ultrastructural alterations of PSCx exposed to different drugs for 4 days were observed under light microscope and SEM. a, d, g The typical morphology and structural integrity of PSCx from the vehicle group; b, e, h The mild morphological and structural alterations in ABZ-SO (20 μg/mL) group. c, f, j Obvious morphological and ultrastructural destructures in PSCx exposed to vepm (20 μg/mL), the disappearance of calcareous corpuscles and hooks, shedding of the tegument and the presence of numerous blebs. a-c Light microscope without any staining (200 × magnification); d-f Light microscope with trypan blue staining (200 × magnification); g-i SEM (600 × magnification). Arrowhead (red) indicates intact calcareous corpuscle.

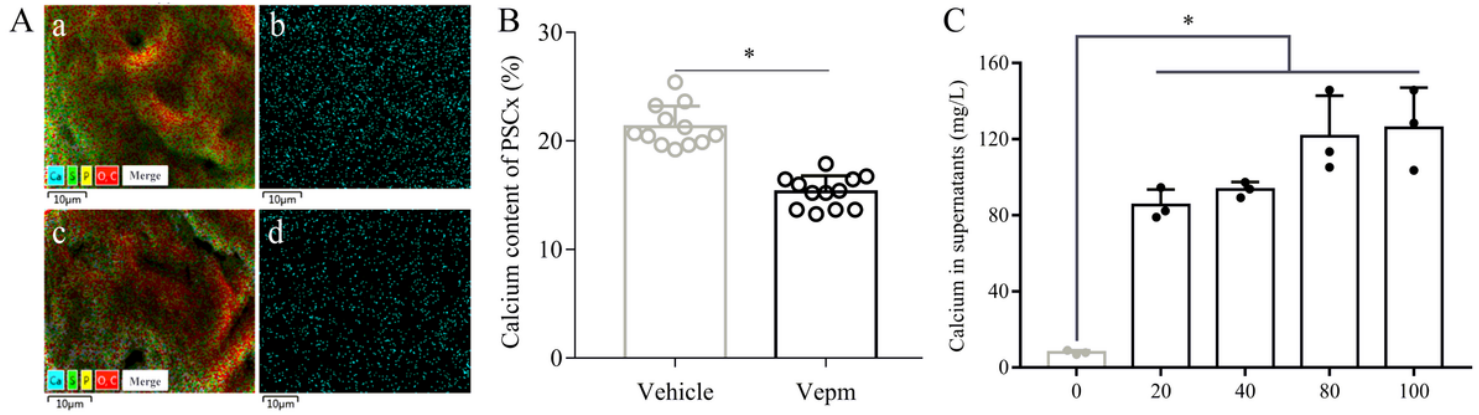

Figure 2

Changes of calcium content in E. granulosus PSCx after treatment with verapamil (vepm) at 20 μg/mL on day 4 in vitro. A. Calcium distribution in E. granulosus PSCx by SEM-EDS. The merge of multi-element (a, c) and calcium (b, d) distribution of PSCx in the vehicle group (a, b) or the vepm group (c, d). B. The percentage of calcium content in E. granulosus PSCx by SEM-EDS. C. The calcium content in culture supernatants of E. granulosus PSCx exposed to vepm (0, 20, 40, 80, 100 μg/mL) by ICP-MS.

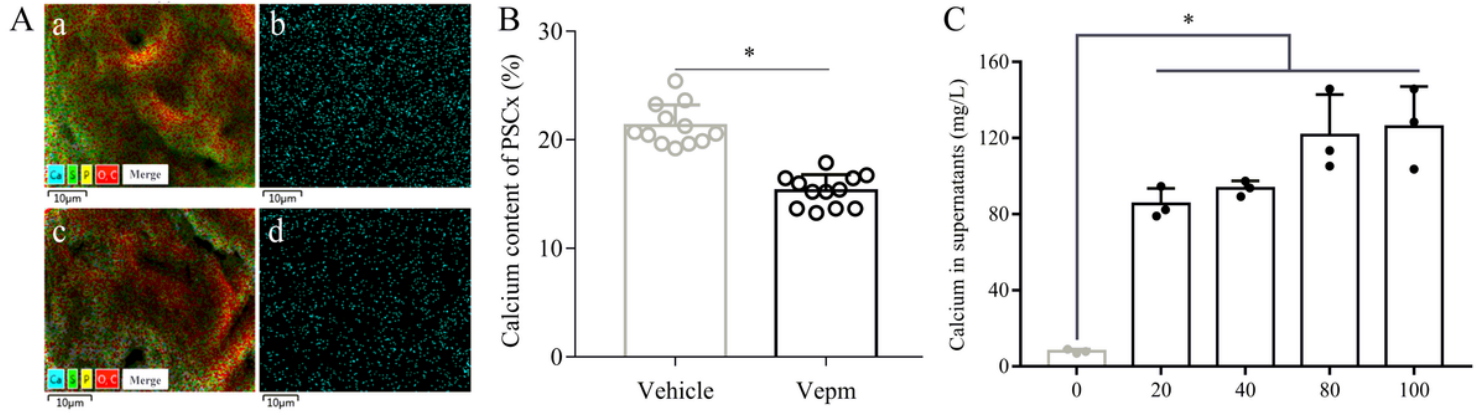

Figure 2

Changes of calcium content in E. granulosus PSCx after treatment with verapamil (vepm) at 20 μg/mL on day 4 in vitro. A. Calcium distribution in E. granulosus PSCx by SEM-EDS. The merge of multi-element (a,

c) and calcium (b, d) distribution of PSCx in the vehicle group (a, b) or the vepm group (c, d). B. The percentage of calcium content in E. granulosus PSCx by SEM-EDS. C. The calcium content in culture supernatants of E. granulosus PSCx exposed to vepm (0, 20, 40, 80, 100 μg/mL) by ICP-MS.

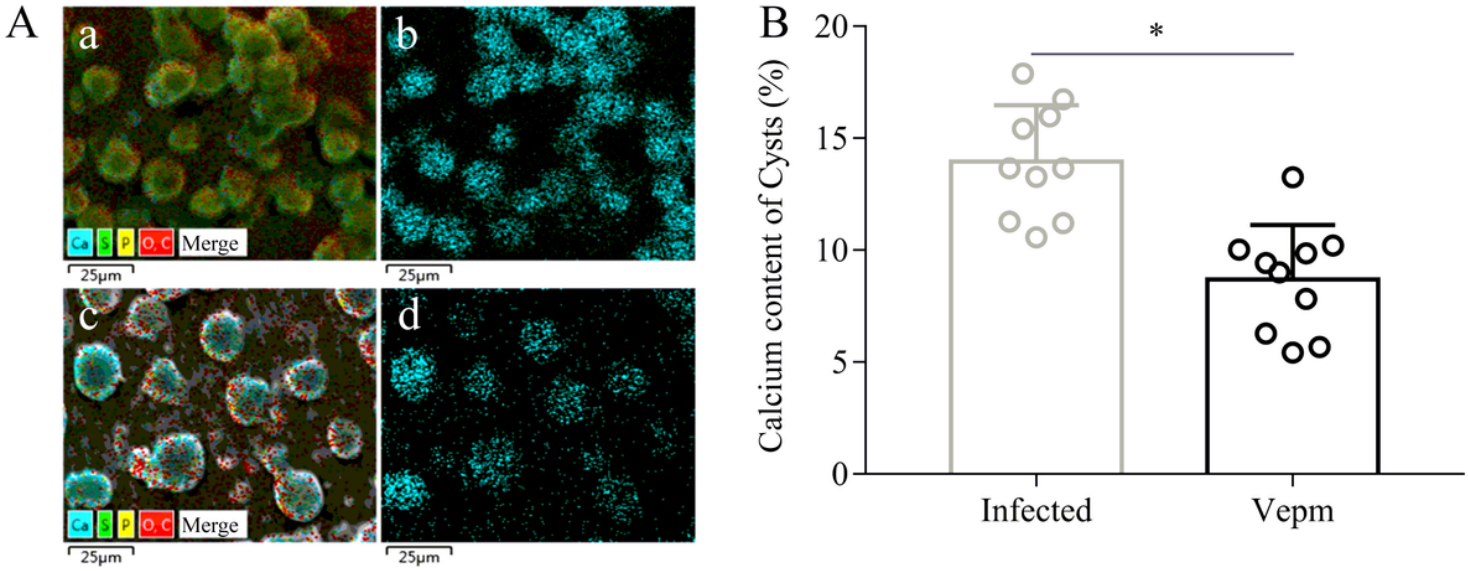

Figure 3

Changes of calcium content of E. multilocularis infected mice after treatment of verapamil (vepm) at 40 mg/kg for 4 months by SEM-EDS. A. Calcium distribution in germinal layer of E. multilocularis cysts. The merge of multi-element (a, c) and calcium (b, d) distribution in germinal layer of the infected group (a, b) or the vepm group (c, d). B. The percentage of calcium content in germinal layer of E. multilocularis metacestodes in mice after treatment of vepm.

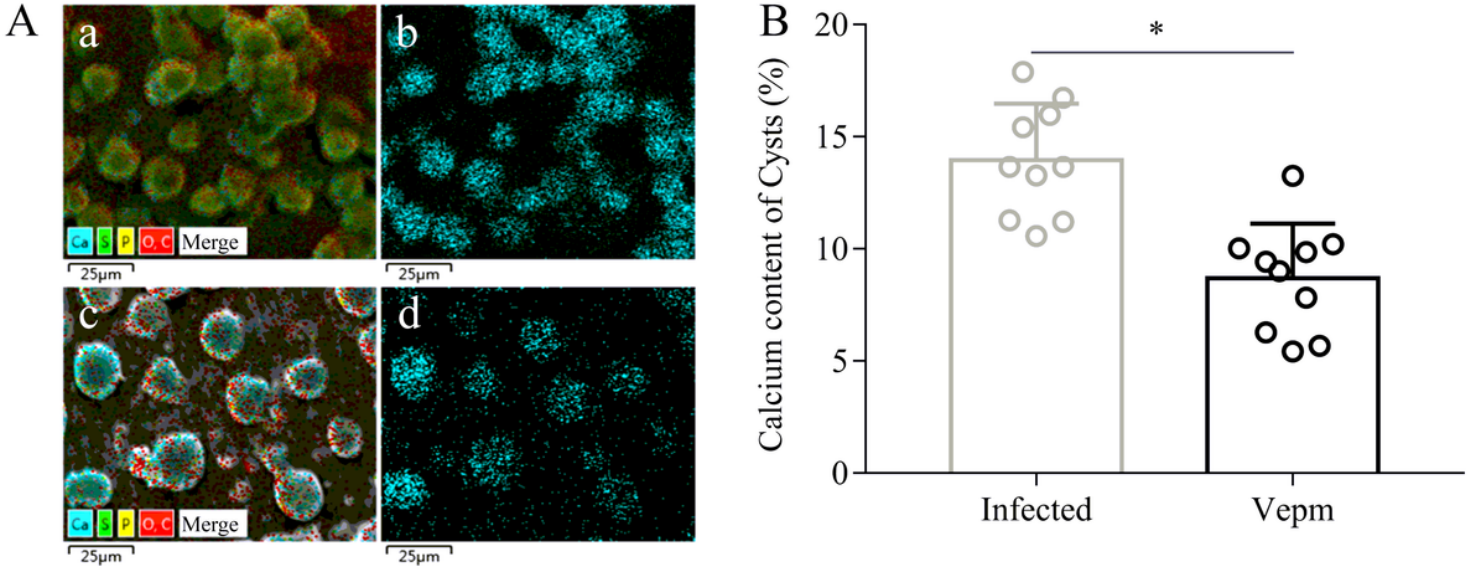

Figure 3

Changes of calcium content of E. multilocularis infected mice after treatment of verapamil (vepm) at 40 mg/kg for 4 months by SEM-EDS. A. Calcium distribution in germinal layer of E. multilocularis cysts. The

merge of multi-element (a, c) and calcium (b, d) distribution in germinal layer of the infected group (a, b) or the vepm group (c, d). B. The percentage of calcium content in germinal layer of E. multilocularis metacestodes in mice after treatment of vepm.

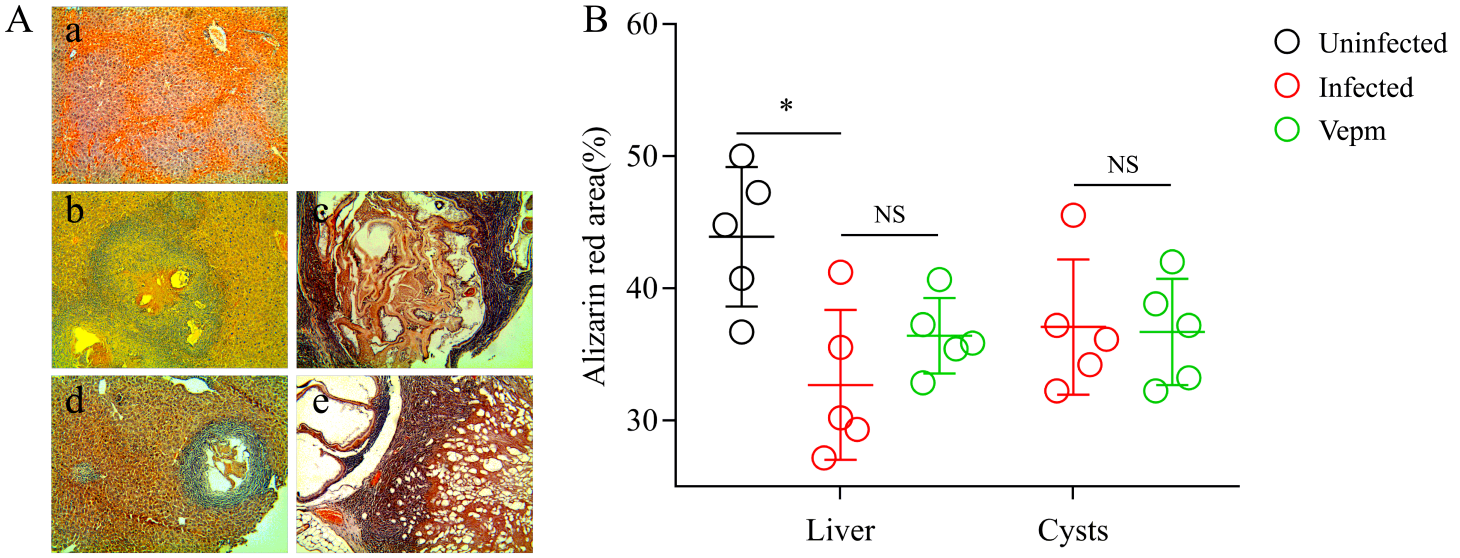

Figure 4

Changes of calcium content of the liver and E. multilocularis cysts in mice after treatment with verapamil (vepm) at 40 mg/kg for 4 months by alizarin red staining. A. Calcium distribution in the liver (a, b, d) and E. multilocularis cysts (c, e) from the uninfected (a), infected (b, c) and vepm (d, e) treated mice (200 × magnification). B. The semi-quantitative analysis of calcium content. NS, no significance.

Figure 4

Changes of calcium content of the liver and E. multilocularis cysts in mice after treatment with verapamil (vepm) at 40 mg/kg for 4 months by alizarin red staining. A. Calcium distribution in the liver (a, b, d) and E. multilocularis cysts (c, e) from the uninfected (a), infected (b, c) and vepm (d, e) treated mice (200 × magnification). B. The semi-quantitative analysis of calcium content. NS, no significance.

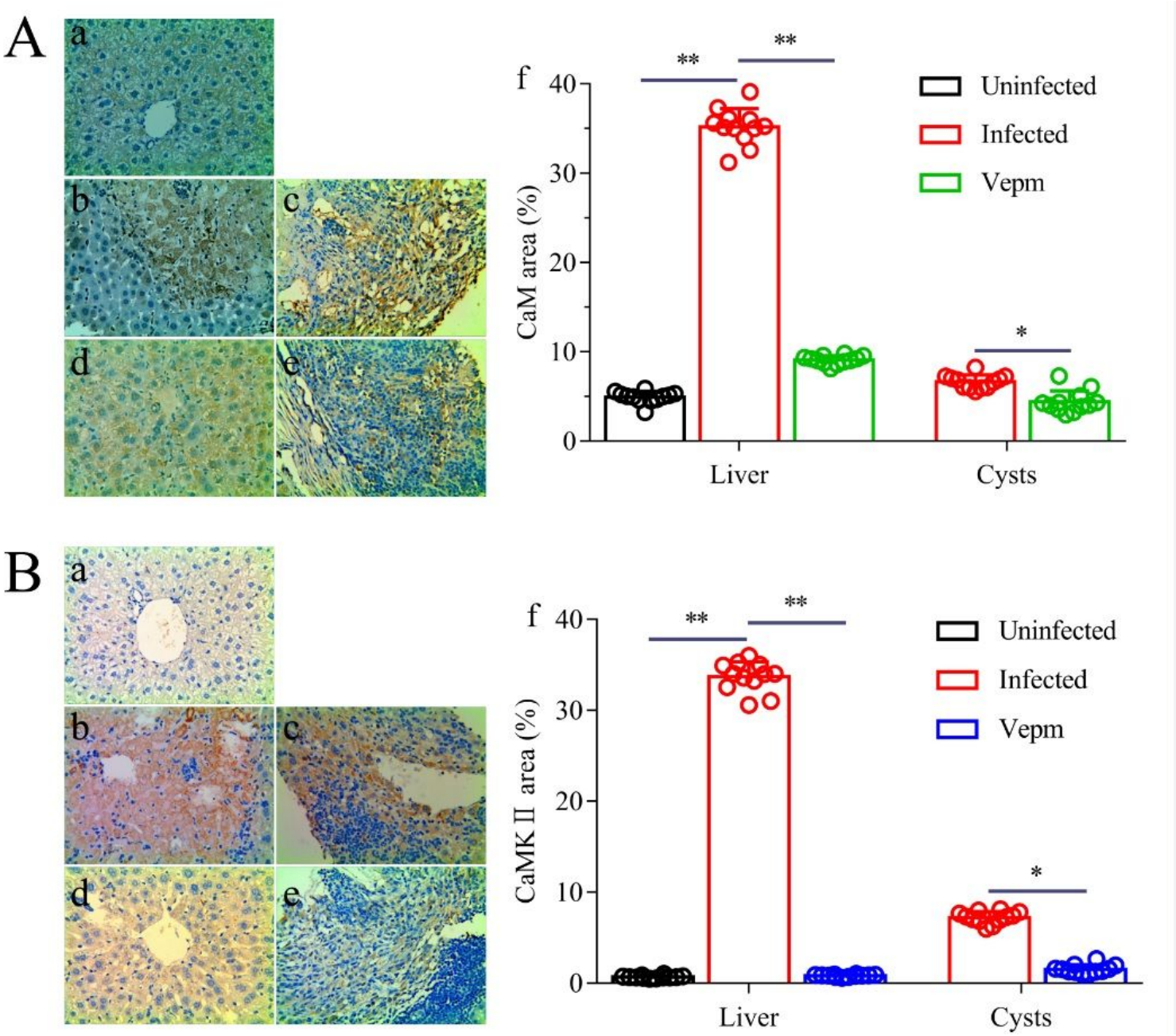

Figure 5

Analysis of CaM and Camk Ⅱ protein expression in the liver and E. multilocularis cysts after treatment with verapamil (vepm) by paraffin-immunohistochemistry. The expression of CaM (A) and CamK Ⅱ (B) protein in liver (a, b, d) and E. multilocularis cysts (c, e) in uninfected (a), infected (b, c) and vepm treated (d, e) mice (400 × magnification). f The semi-quantitative analysis of CaM and CamK Ⅱ protein expression.

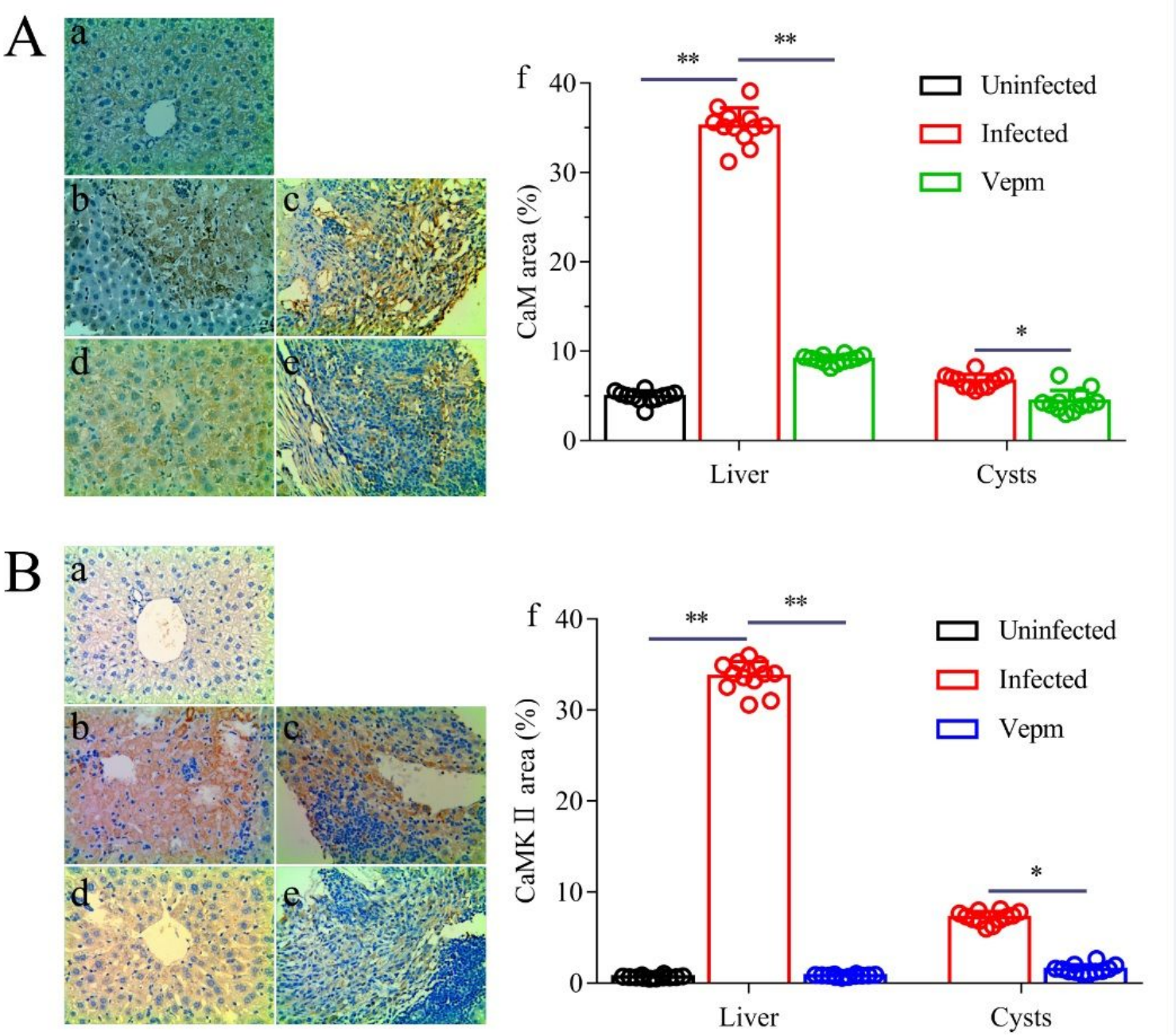

Figure 5

Analysis of CaM and Camk Ⅱ protein expression in the liver and E. multilocularis cysts after treatment with verapamil (vepm) by paraffin-immunohistochemistry. The expression of CaM (A) and CamK Ⅱ (B) protein in liver (a, b, d) and E. multilocularis cysts (c, e) in uninfected (a), infected (b, c) and vepm treated (d, e) mice (400 × magnification). f The semi-quantitative analysis of CaM and CamK Ⅱ protein expression.

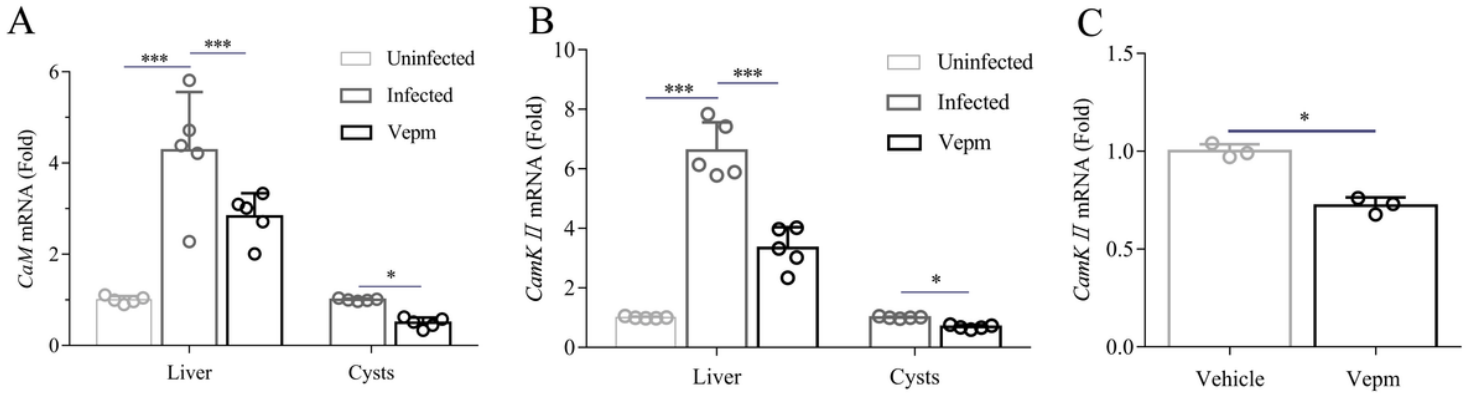

Figure 6

Expression of CaM and Camk Ⅱ mRNA in the liver and E. multilocularis cysts from mice after treatment with verapamil (vepm) at 40mg/kg for 4 months and E. granulosus PSCx after exposed to vepm (20 μg/mL) for 4 days by RT-qPCR. A. CaM mRNA expression. B. CamK Ⅱ mRNA expression. C. CamK Ⅱ mRNA expression in E. granulosus PSCx.

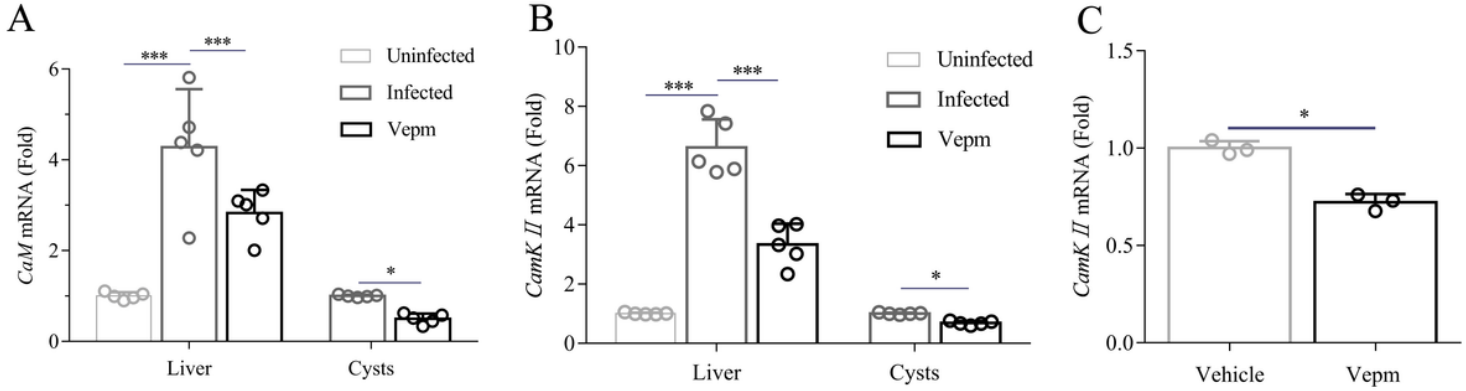

Figure 6

Expression of CaM and Camk Ⅱ mRNA in the liver and E. multilocularis cysts from mice after treatment with verapamil (vepm) at 40mg/kg for 4 months and E. granulosus PSCx after exposed to vepm (20 μg/mL) for 4 days by RT-qPCR. A. CaM mRNA expression. B. CamK Ⅱ mRNA expression. C. CamK Ⅱ mRNA expression in E. granulosus PSCx.

Supplementary Files

This is a list of supplementary files associated with this preprint. Click to download.

- GraphicAbstract.tif
- GraphicAbstract.tif